Optimal Controller Design of Three-Phase Controlled Rectifier Using Artificial Intelligence Techniques

Koson Chaijarurnudomrung[1], **Kongpan Areerak**[2], **Kongpol Areerak**[3], and **Umaporn Kwannetr**[4], Non-members

ABSTRACT

This paper presents a controller design for a three-phase controlled rectifier using artificial intelligence techniques to regulate the DC-bus voltage. The averaging model of the power electronic system is used as an objective function instead of the model from software packages. The averaging model is derived from the DQ modeling approach in which the dynamics of the transmission line and power converter are taken into account for the controller design. The results show that the proposed method can efficiently obtain the best performance of the output waveform compared with the classical method. Moreover, this approach is convenient and flexible for electrical engineering to design the controller of power electronic systems with the best output performance.

Keywords: Three-Phase Controlled Rectifier, Averaging model, DQ modeling method, Adative Tabu Search, Artificial Bee Colony

1. INTRODUCTION

Presently, the artificial intelligence (AI) techniques are widely applied to many works of engineering such as the system identifications using adaptive tabu search (ATS) [1]-[5], the protection design in power system via ATS [6], the active power filter design using genetic algorithm (GA) [7], power loss minimization using particle swarm optimization (PSO) and artificial bee colony (ABC) [8], reactive power optimization for distribution systems based on ant colony optimization (ACO) [9], and etc. In this paper, the AI technique called ATS and ABC are used for the controller design of three-phase controlled rectifier. The controllers of this power system are used to regulate the DC-link voltage. Therefore, the ATS and ABC are applied to search the PI controller parameters to achieve the best output performance. However, when the AI is applied to the power electronic system, the main problem is the simulation time. This is because the simulation of power electronic system using software packages (such as MATLAB, PSIM, and etc.) provide a huge simulation time due to a switching behavior. It is not easily applicable for the AI search method. To solve this problem, the averaging model of the system is used to simulate the system instead of the exact topology model via the simulation software packages. The works from this paper also show the application of mathematical model derived from the DQ modeling method for the searching method in which it has not been reported in the previous publications. From [10]-[13], the DQ modeling method is used to derive the mathematical model of three-phase system for the stability analysis. In this paper, the DQ model of three-phase controlled rectifier is applied to the controller design using ATS and ABC methods in which the DQ model is used as the objective function. In addition, the advantage of the proposed averaging model is that the dynamics of transmission line and power converter are taken into account for the controller design. In contrast, these dynamics are not considered when the controllers are designed by the classical method. The paper is structured as follows. In Section 2, the considered system definition and deriving the dynamic model for the controller design using AI techniques are explained. The controller design using ATS and ABC methods is explained in Section 3. The simulation results using the controllers design from the proposed techniques are presented in Section 4. Finally, Section 5 concludes and discusses the advantages of the proposed model for the system design compared with the classical method.

2. CONSIDERED SYSTEM

The studied power system in the paper is depicted in Fig.1. It consists of a balanced three-phase voltage source, transmission line, three-phase controlled rectifier, and DC-link filters feeding a constant power load (CPL). The controllers of the power system in Fig.1 are used to keep the voltage across the DC-link capacitor constant, here regulated to the V_{out}^{*} voltage command. The system parameters of Fig.1 are V_s = 230 $V_{\text{rms/phase}}$, f=50 Hz, R_{eq}= 0.1 Ω, L_{eq}=24 μH, C_{eq}= 2nF, C_F=1000 μF, r_F=0.03 Ω, and L_F=6.5

Manuscript received on July 28, 2011 ; revised on September 28, 2011.

[1,2,3,4] The authors are with the School of Electrical Engineering, Suranaree University of Technology Nakhon Ratchasima, 30000, Thailand, E-mail:koson_ee@hotmail.com, kongpan@sut.ac.th, kongpol@sut.ac.th and muayja1@hotmail.com

[2] Corresponding author

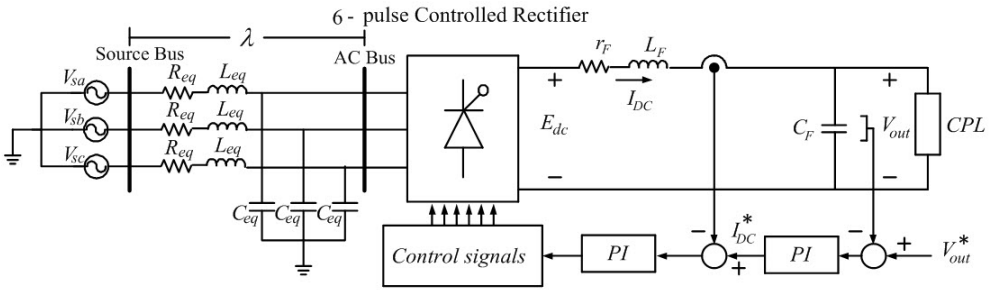

Fig.1: *The considered power system*

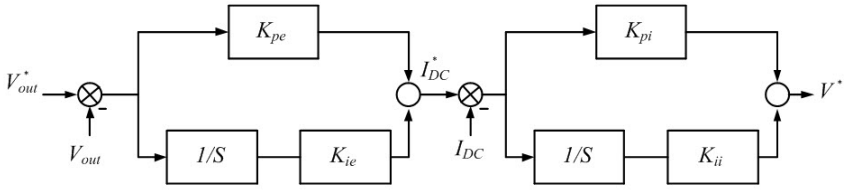

Fig.2: *The schematic of controllers*

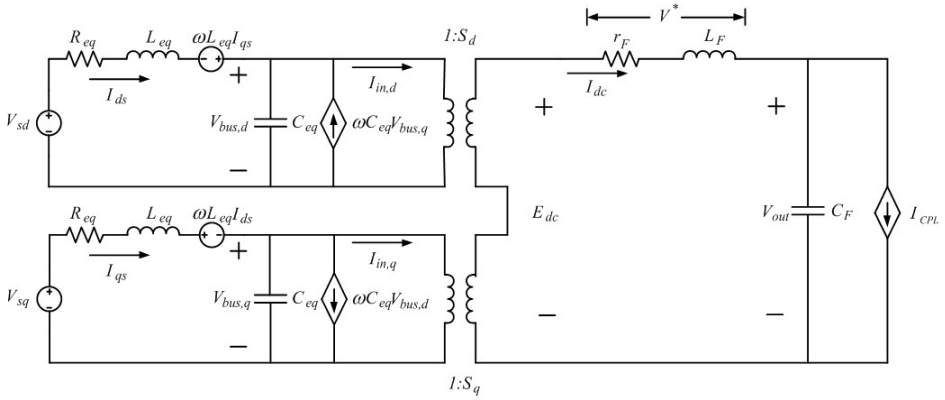

Fig.3: *The equivalent circuit of the system in Fig. 1 on DQ frame*

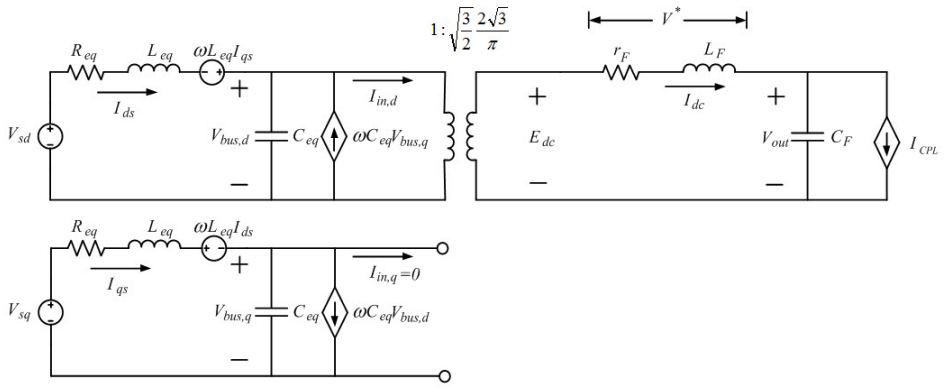

Fig.4: *The simplified equivalent circuit of the power system*

mH. The schematic of the controllers of the system in Fig.1 is shown in Fig.2. The parameters K_{pe}, K_{ie}, K_{pi}, K_{ii} are the proportional and integral gains of voltage and current PI controllers, respectively. In this paper, the design of these controllers using the classical, ATS, and ABC methods is presented. The comparison results between the systems using the controllers designed from the different techniques are also shown.

The work in [13] described the equivalent circuit of the power system in Fig. 1 on DQ frame without the controllers as depicted in Fig. 3. The equivalent circuit in Fig. 3 can be simplified by fixing the rotating frame on the phase of the switching function. This results in the circuit as shown in Fig. 4. As mentioned in Section 1, the mathematical model of the power system will be used as the objective function for ATS and ABC methods in the paper to reduce the simulation time. However, the controllers are not considered in the DQ model in [13]. Therefore, if we would like to use the DQ model as the objective function in the paper, the controllers will be considered into the model. To consider the controllers of the system, from Fig. 2, PI controller output V^* can be derived and given by:

$$\left.\begin{aligned} V^* = &-K_{pi}I_{dc} - K_{pe}K_{pi}V_{out} + K_{ie}K_{pi}X_v + K_{ii}X_i \\ &+ K_{pe}K_{pi}V^*_{out} \end{aligned}\right\} \quad (1)$$

According to Fig. 2, the differential equations of X_v and X_i can be written as:

$$\left.\dot{X}_e = -V_{out} + V^*_{out}\right\} \quad (2)$$

$$\left.\dot{X}_i = -I_{dc} - K_{pe}V_{out} + K_{ie}X_e + K_{pe}V^*_{out}\right\} \quad (3)$$

According to Fig. 4, when the power system is controlled, the voltage across the r_F and L_F is equal to V^*. Hence, this voltage can be written by:

$$\left.r_F I_{dc} + L_F \dot{I}_{dc} = V^*\right\} \quad (4)$$

Substituting Eq. (1) into Eq. (4), the differential equation of I_{dc} becomes

$$\left.\begin{aligned} \dot{I}_{dc} = &-\left(\frac{r_F + K_{pi}}{L_F}\right) I_{dc} + \frac{K_{ie}K_{pi}}{L_F}X_e + \frac{K_{ii}}{L_F}X_i \\ &- \frac{K_{pe}K_{pi}}{L_F}V_{out} + \frac{K_{pe}K_{pi}}{L_F}V^*_{out} \end{aligned}\right\} \quad (5)$$

Applying the Kirchhoff's voltage law (KVL) and the Kirchhoff's current law (KCL) to the circuit in Fig. 4 with (2), (3), and (5) obtains the set of nonlinear differential equations as follows the equation (6)

The equation (6) is a nonlinear equation. Therefore, (6) is linearized using the first order terms of the Taylor's series expansion so as to achieve a set of linear differential equations around an equilibrium point. The DQ linearized model of (6) is then of the following form the equation (7)

$$\left.\begin{aligned} \dot{I}_{ds} &= -\frac{R_{eq}}{L_{eq}}l_{ds} + \omega I_{qs} - \frac{1}{L_{eq}}V_{bus,d} + \frac{1}{L_{eq}}V_{sd} \\ \dot{I}_{qs} &= -\omega I_{ds} - \frac{R_{eq}}{L_{eq}}I_{qs} - \frac{1}{L_{eq}}V_{bus,q} + \frac{1}{L_{eq}}V_{sq} \\ \dot{V}_{bus,d} &= \frac{1}{C_{eq}}I_{ds} + \omega V_{bus,q} - \sqrt{\frac{3}{2}}\cdot\frac{2\sqrt{3}}{\pi C_{eq}}I_{dc} \\ \dot{V}_{bus,q} &= -\omega V_{bus,d} + \frac{1}{C_{eq}}I_{qs} \\ \dot{I}_{dc} &= -\left(\frac{r_F + K_{pi}}{L_F}\right)I_{dc} + \frac{K_{ie}K_{pi}}{L_F}X_e + \frac{K_{ii}}{L_F}X_i \\ &- \frac{K_{pe}K_{pi}}{L_F}V_{out} + \frac{K_{pe}K_{pi}}{L_F}V^*_{out} \\ \dot{V}_{out} &= \frac{1}{C_F}I_{dc} - \frac{1}{C_F}\frac{P_{CPL}}{V_{out}} \\ \dot{X}_e &= -V_{out} + V^*_{out} \\ \dot{X}_i &= -I_{dc} - K_{pe}V_{out} + K_{ie}X_e + K_{pe}V^*_{out} \end{aligned}\right\} \quad (6)$$

$$\left.\begin{aligned} \delta\dot{\mathbf{x}} &= \mathbf{A}(\mathbf{x_o}, \mathbf{u_o})\delta\mathbf{x} + \mathbf{B}(\mathbf{x_o}, \mathbf{u_o})\delta\mathbf{u} \\ \delta\mathbf{y} &= \mathbf{C}(\mathbf{x_o}, \mathbf{u_o})\delta\mathbf{x} + \mathbf{D}(\mathbf{x_o}, \mathbf{u_o})\delta\mathbf{u} \end{aligned}\right\} \quad (7)$$

Where

$$\delta\mathbf{x} = [\delta I_{ds}\ \delta I_{qs}\ \delta V_{bus,d}\ \delta V_{bus,q}\ \delta I_{dc}\ \delta V_{out}\ \delta X_e\ \delta X_i]^T$$

$$\delta\mathbf{u} = [\delta V_m\ \ \delta V^*_{out}\ \ \delta P_{CPL}]^T, \quad \delta\mathbf{y} = [\delta V_{out}]$$

The details of $\mathbf{A}(\mathbf{x_o}, \mathbf{u_o})$, $\mathbf{B}(\mathbf{x_o}, \mathbf{u_o})$, $\mathbf{C}(\mathbf{x_o}, \mathbf{u_o})$, and $\mathbf{D}(\mathbf{x_o}, \mathbf{u_o})$ are:

It can be seen in Eq. (7) that the PI controller parameters appear in the linearized model in which these parameters are not appeared in the model of the work in [13]. The model including the controller parameters will be used as an objective function for the ATS and ABC algorithms that will be explained in Section 3.

The DQ linearized model in Eq. (7) needs to define V_{out},λ_o, and α_o. The power flow equation can be applied to determine the steady state value at the AC side of the power system in Fig. 1. This leads to a system of nonlinear equations:

$$\left.\frac{V_s V_{bus}}{Z}\cos(\gamma - \lambda) - \frac{V^2_{bus}}{Z}\cos(\gamma) = P_{bus}\right\} \quad (8)$$

$$\left.\frac{V_s V_{bus}}{Z}\sin(\gamma - \lambda) - \frac{V^2_{bus}}{Z}\sin(\gamma) = Q_{bus}\right\} \quad (9)$$

where the following steady-state values are: $V_{bus,o}$ - voltage at AC bus (rms), λ_o - phase shift between

$$\mathbf{A}(\mathbf{x}_o,\mathbf{u}_o)=\begin{bmatrix} -\frac{R_{eq}}{L_{eq}} & \omega & -\frac{1}{L_{eq}} & 0 & 0 & 0 & 0 & 0 \\ -\omega & -\frac{R_{eq}}{L_{eq}} & 0 & -\frac{1}{L_{eq}} & 0 & 0 & 0 & 0 \\ \frac{1}{C_{eq}} & 0 & 0 & \omega & \sqrt{\frac{3}{2}}\cdot\frac{2\sqrt{3}}{\pi C_{eq}} & 0 & 0 & 0 \\ 0 & \frac{1}{C_{eq}} & -\omega & 0 & 0 & 0 & 0 & 0 \\ 0 & 0 & 0 & 0 & -\frac{(r_F+K_{pi})}{L_F} & -\frac{(K_{pe}K_{pi})}{L_F} & \frac{K_{ie}K_{pi}}{L_F} & \frac{K_{ii}}{L_F} \\ 0 & 0 & 0 & 0 & \frac{1}{C_F} & \frac{P_{CPL}}{C_F V_{out,o}^2} & 0 & 0 \\ 0 & 0 & 0 & 0 & 0 & -1 & 0 & 0 \\ 0 & 0 & 0 & 0 & -1 & -K_{pe} & K_{ie} & 0 \end{bmatrix}_{8\times 8}$$

$$\mathbf{B}(\mathbf{x}_o,\mathbf{u}_o)=\begin{bmatrix} \sqrt{\frac{3}{2}}\cdot\frac{\cos(\lambda_o+\alpha)}{L_{eq}} & 0 & 0 \\ \sqrt{\frac{3}{2}}\cdot\frac{\sin(\lambda_o+\alpha)}{L_{eq}} & 0 & 0 \\ 0 & 0 & 0 \\ 0 & 0 & 0 \\ 0 & \frac{K_{pe}K_{pi}}{L_F} & -\frac{1}{C_F V_{out,o}} \\ 0 & 0 & 0 \\ 0 & 1 & 0 \\ 0 & K_{pe} & 0 \end{bmatrix}_{8\times 3}$$

$$\mathbf{C}(\mathbf{x}_o,\mathbf{u}_o)=\begin{bmatrix}0 & 0 & 0 & 0 & 0 & 1 & 0 & 0\end{bmatrix}_{1\times 8}\quad \mathbf{D}(\mathbf{x}_o,\mathbf{u}_o)=\begin{bmatrix}0 & 0 & 0\end{bmatrix}_{1\times 3}$$

V_s and V_{bus}. Note that $Z\angle\gamma$ is the transmission line impedance, while the active and reactive power (per phase) at the AC bus is given by:

$$P_{bus}=V_{bus}I_{bus}\cos\alpha\Big\} \tag{10}$$

$$Q_{bus}=V_{bus}I_{bus}\sin\alpha\Big\} \tag{11}$$

where

$$P_{bus}=\frac{P_{CPL}+P_{loss}}{3}\Big\} \tag{12}$$

$$Q_{bus}=\frac{P_{CPL}+P_{loss}}{3}\tan(\alpha)\Big\} \tag{13}$$

In (12), P_{CPL} is the constant power load value and P_{loss} is the power loss due to r_F. In addition, it can be seen in (13) that the reactive power Q_{bus} depends on the firing angle α in which this angle can be calculated by:

$$\alpha=\cos^{-1}\left(\frac{\pi V_{out}^*}{3\sqrt{3}(\sqrt{2}V_{bus})}\right)\Big\} \tag{14}$$

Substituting α in (14) into (13) to yield

$$Q_{bus}=\frac{(P_{CPL}+P_{loss})\tan\left(\cos^{-1}\left(\frac{\pi V_{out}^*}{3\sqrt{3}(\sqrt{2}V_{bus})}\right)\right)}{3}\Big\} \tag{15}$$

Applying P_{bus} in (10) and Q_{bus} in (11) into (8) and (9), respectively, the power flow equations can be written as:

$$\frac{V_sV_{bus}}{Z}\cos(\gamma-\lambda)-\frac{V_{bus}^2}{Z}\cos(\gamma)=\frac{(P_{CPL}+P_{loss})}{3}\Big\} \tag{16}$$

$$\frac{V_sV_{bus}}{Z}\sin(\gamma-\lambda)-\frac{V_{bus}^2}{Z}\sin(\gamma)=\frac{(P_{CPL}+P_{loss})\tan\left(\cos^{-1}\left(\frac{\pi V_{out}^*}{3\sqrt{3}(\sqrt{2}V_{bus})}\right)\right)}{3} \tag{17}$$

Equations (16) and (17) can be solved by using a numerical method such as Newton Raphson to achieve $V_{bus,o}$ and λ_o at the steady-state conditions. Consequently, $V_{out,o}$ and α_o for DQ linearized model in Eq. (7) can then be calculated by

$$V_{out,o}=V_{out}^*\} \tag{18}$$

$$\alpha_o=\cos^{-1}\left(\frac{\pi V_{out}^*}{3\sqrt{3}(\sqrt{2}V_{bus,o})}\right)\Big\} \tag{19}$$

Before using the DQ linearized model in Eq. (7), it has to be validated by the intensive time-domain simulation called the benchmark model as shown in Fig 5. The simulation for model validation uses the exact topology model in SimPowerSystemTM of SIMULINK with the system parameters and the PI controller parameters designed by the classical method that are K_{pv} = 0.101, K_{iv} = 3.9478, K_{pi} = 4.5442, and K_{ii} = 1257.4. Fig. 6 shows the comparison of V_{out} response between the DQ linearized model and the benchmark model to a step change of P_{CPL} from 7 to 8kW that occurs at t = 1 s., here the voltage command V_{out}^* is set to 500 V.

From the results in Fig. 6, an excellent agreement between both models is achieved under small-signal simulation. It confirms that the mathematical model of a controlled rectifier with its control derived from the DQ method can accurately explain the system dynamic behavior. Therefore, this model can then be used for the controller design using the ATS and ABC methods that will be explained in Section 3. It can be seen that the controller parameters K_{pe}, K_{ie}, K_{pi}, K_{ii} occur in the model as given in (7). Hence,

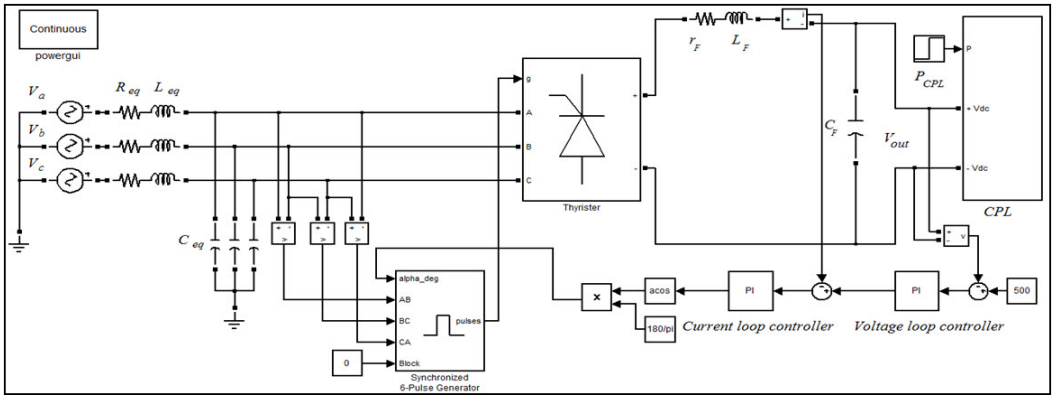

Fig.5: *The benchmark model of the system in Fig.1*

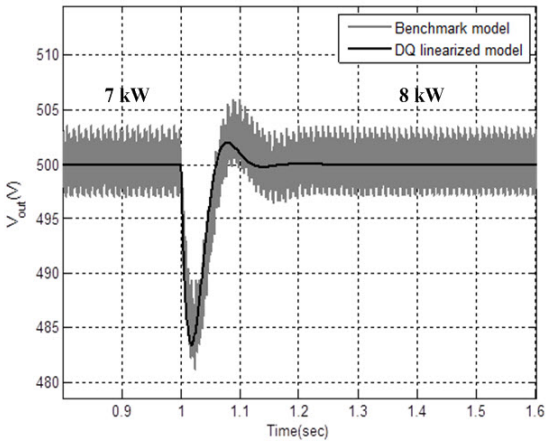

Fig.6: *Model verification for changing P_{CPL} from 7 to 8kW (V^*_{out} = 500 V)*

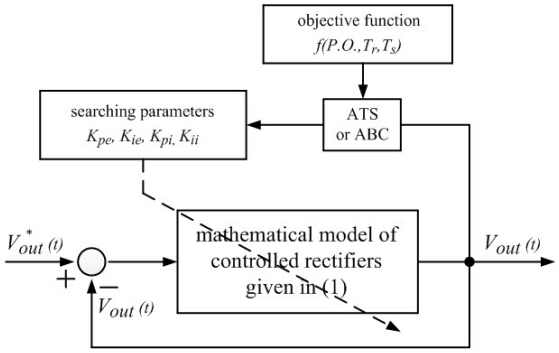

Fig.7: *The AI methods for the PI controller design*

the ATS and ABC algorithms will search the appropriate controllers to achieve the best performance of the system responses. Note that the simulation using the exact topology model via the simulation software packages is replaced by the DQ model as given in (7). The system simulation using (7) can be easily programmed on the M-file of MATLAB. Without the model in (7), the software package such as SimPowerSystem^{TM} in SIMULINK can be used in which the switching behaviors are taken into account in the simulation. The simulation including the switching action of the device consumes the huge simulation time. Therefore, in this paper, the DQ linearized model is reasonably selected below.

3. CONTROLLER DESIGN USING ATS AND ABC METHODS

The controller design using the ATS and ABC searching methods is briefly explained in this section. The block diagram to explain how to search the PI controller parameters using ATS and ABC methods is shown in Fig.7.

It can be seen in Fig.7 that ATS or ABC methods will search the controller parameters K_{pe}, K_{ie}, K_{pi}, K_{ii} in which the objective value (W) is defined by

$$W(T_R, T_S, P.O.) = \sigma T_R + \alpha T_S + \gamma P.O.\} \qquad (20)$$

and

$$\sigma + \alpha + \gamma = 1\} \qquad (21)$$

$P.O.$ is the percent overshoot of the V_{out} response.
T_R is the rise time of the V_{out} response.
T_S is the setting time of the V_{out} response
σ, α, and γ are the priority coefficients of T_R, T_S, and $P.O.$, respectively.

In this paper, the values of σ, α, and γ are set to 0.33, 0.33, and 0.34, respectively. The ATS and ABC searching methods will try to search the best controller parameters until the minimum W is achieved. This means the controller parameters from the searching provide the best performance of V_{out} response.

3.1 Adaptive Tabu Search (ATS)

The ATS algorithm is developed by K-N. Areerak and S. Sujitjorn in 2002 [1]. This algorithm guarantees the optimal solution for the searching process.

According to Fig.7, the steps of searching controller parameters by using ATS are as follows:

Step 1: Determine the boundary of parameters, radius value (R: the one of ATS parameters), maximum of searching iteration (Countmax). In this paper, the upper and lower limits of K_{pe}, K_{ie}, K_{pi}, K_{ii} are set to [0.101 0.201], [3.94 15.79], [1.27 3.23], [102.64 641.52], respectively. These boundary values are calculated by using $\omega_{ni} = 2\pi \times 20$ to $2\pi \times 50$ rad/s and $\omega_{ne} = 2\pi \times 10$ to $2\pi \times 20$ rad/s with the constant $\zeta = 0.8$ and the system parameters as defined in Section 2. Note that ni is the bandwidth of current loop control, while ne is the bandwidth of voltage loop control.

Step 2: Random the initial value for each parameter (S_0) within the search space as defined from *Step*1 and define S_0 is the best solution in the search space (*best_neighbor*).

Step 3: Random the N solutions (N neighborhood) around S0 in the search space with radius equal to R. After that, define the set of N solutions is $S(R)$.

Step 4: Evaluate the solutions in $S(R)$ with the objective function as defined in (2) and define S_1 (*best_neighbor1*) is the best solution in $S(R)$. Note that the best solution means the solution that can provide the minimum value of W. The W value can be calculated from (20) in which it depends on the output voltage response.

Step 5: If $S_1 < S_0$ then define $S_0 = S_1$ and keep S_0 in the tabu list.

Step 6: If $count \geq count_{max}$ then stop the ATS searching and S_0 is the best solution. However, the ATS still search the solution if $count < count_{max}$ by start the *Step 3* again. In this step, the back tracking process is used to escape the local solution.

Step 7: Adjust the radius of search space with the decreasing factor (DF) by

$$radius_{new} = \frac{radius_{old}}{DF} \Bigg\} \tag{22}$$

Note that the more details of ATS algorithm can be found in [1]-[6].

3.2 Artificial Bee Colony (ABC)

The ABC algorithm is based on the behavior of honey bee swarms. According to Fig. 7, the steps of searching controller parameters by using ABC algorithm are as follows:

Step 1: Determine the boundary of the search space. The lower and upper limits of controller parameters are set equal to those of ATS method.

Step 2: Define the colony size.

Step 3: Define the numbers of searching parameters where they are appeared in the objective function. For this work, they are equal to 4 parameters: K_{pe}, K_{ie}, K_{pi}, and K_{ii}.

Step 4: Random the initial value of artificial bee within the search space by using

$$x_{ij} = x_{min,j} + rand(0,1) \times (x_{max,j} - x_{min,j})\} \tag{23}$$

where

$x_{min,j}$ is the minimum value of parameter j

$x_{max,j}$ is the maximum value of parameter j

Step 5: Evaluate the W values of the population by using the following equation:

$$pf_i = \frac{f_{iti}}{\sum_{j=1}^{n} f_{iti}} \Bigg\} \tag{24}$$

where pf_j is the probability value for an artificial bee j.The f_{iti} in (24) can be calculated by using:

$$f_{iti} = \left\{ \begin{array}{ll} \frac{1}{1+f_i} & , f_i \geq 0 \\ 1 + abs(f_i) & , f_i < 0 \end{array} \right\} \tag{25}$$

where f_i is the W value for an artificial bee j.

Step 6: Determine the maximum of searching iteration ($iteration_{max}$).

Step 7: If $iteration < iteration_{max}$, go to Step 4 again.

4. SIMULATION RESUITS

In this section, the system as shown in Fig.1 having the controllers designed by using ATS and ABC is simulated by using PSB in SIMULINK to compare the simulation results with the classical method as described in Appendix. The aim of the ATS and ABC approaches is to minimize the W value to achieve the best output response. The comparison results of the controller parameters that are designed from the difference methods are given in Table 1.

Table 1: *The Comparison Between ATS,ABC and Classical Methods*

Controller Parameter	Design Method		
	ATS Method	ABC Method	Classical Method
K_{pe}	0.2006	0.198	0.101
K_{ie}	15.6866	12.5363	3.9478
K_{pi}	2.8297	3.2802	3.237
K_{ii}	536.8692	510.4455	641.524
W	1.2557	1.2825	2.4094

It can be seen in Table 1 that the controllers designed from the ATS and ABC methods obtain the minimum W value compared with the W value of the classical method. The power system in Fig.1 is simulated with the system parameters and the controller parameters from the ATS, ABC, and classical methods. The details of classical method for controller

design can be found in Appendix. Fig. 8 shows the V_{out} response to a step change of CPL from 7 kW to 9 kW that occurs at $t = 0.5$ s. For this case, the command input V^*_{out} is set to 500 V.

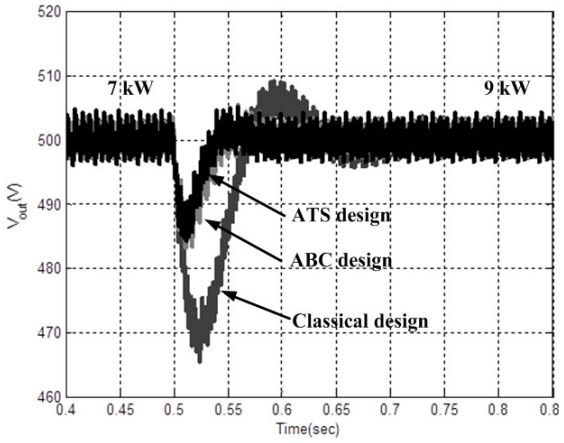

Fig.8: *Simulation results for ATS, ABC, and classical method*

In Fig.8, it can be seen that the output response from the ATS and ABC designs is better than that from the classical design in terms of percent overshoot, rise time and setting time. In addition, The convergences of W value from the ATS and ABC searches are depicted in Fig.9 and Fig. 10, respectively.

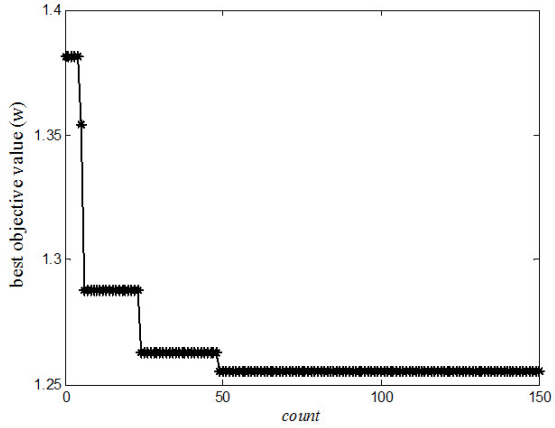

Fig.9: *The convergence of W value from ATS method*

5. CONCLUSIONS

This paper presents the applications of both ATS and ABC algorithms with the DQ linearized model for the design of three-phase controlled rectifier. The dynamics of transmission line and power converter are also taken into account in the proposed design process in which these dynamics are not normally

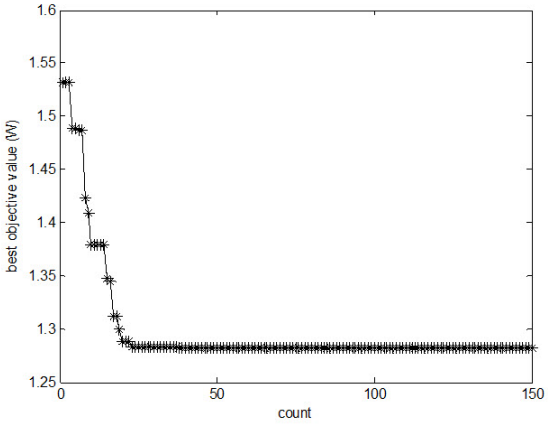

Fig.10: *The convergence of W value from ABC method*

concerned for the controller design by using the classical method. The results confirm that both ATS and ABC methods can provide the best performance of the output response compared with the result from the classical method. However, the controller design using ATS and ABC methods for the power electronic system needs the mathematical model of the system. This is because the simulation of power electronic system using software packages consumes a huge simulation time due to a switching behavior. The work in this paper shows that the proposed method is very convenient and flexible for the controller design of power electronic system with the best system performance.

6. ACKNOWLEDGEMENT

The authors would like to acknowledge National Science and Technology Development Agency (NSTDA) and Suranaree University of Technology (SUT), Thailand, for financial support during the research of the work described in this paper.

7. APPENDIX

The details of classical method for PI controller design are as follow:

- Current loop control

The schematic of the current loop control of the system in Fig.1 is shown in Fig.A1

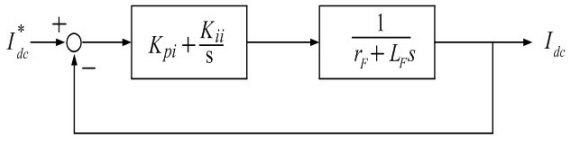

Fig.A1*: current loop control*

In Fig.A1., the K_{pi} and K_{ii} are the PI parameters of current loop control, while R_F and L_F are the DC-

link filter parameters. Closed loop transfer function of the current loop is given by:

$$\left.\frac{I_{dc}}{I_{dc}^*} = \frac{sK_{pi} + K_{ii}}{s^2 + \left(\frac{K_{pi}+r_F}{L_F}\right)s + \frac{K_{ii}}{L_F}}\right\} \quad \text{(A-1)}$$

The closed loop denominator has roots with ω_{ni} and ζ. The standard second order form is

$$\left. s^2 + 2\zeta\omega_n s + \omega_n^2 \right\} \quad \text{(A-2)}$$

Hence, the current loop controller can be designed by comparing between the denominator of (A-1) and (A-2) to yield:

$$\left. K_{pi} = 2\zeta\omega_{ni}L_F - r_F \right\} \quad \text{(A-3)}$$

$$\left. K_{ii} = \omega_{ni}^2 L_F \right\} \quad \text{(A-4)}$$

- Voltage loop control

The schematic of the voltage loop control of the system in Fig.1 is shown in Fig.A2

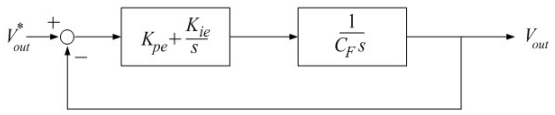

***Fig.A2**: voltage loop control*

In Fig.A2., the K_{pe} and K_{ie} are the PI parameters of voltage loop control, while C_F is the DC-link capacitor. Closed loop transfer function of the voltage loop is given by:

$$\left.\frac{V_{out}}{V_{out}^*} = \frac{sK_{pe} + K_{ie}}{s^2 + \frac{K_{pe}}{C_F}s + \frac{K_{ie}}{C_F}}\right\} \quad \text{(A-5)}$$

Therefore, the voltage loop controller can be designed by comparing between the denominator of (A-5) and (A-2) to yield:

$$\left. K_{pe} = 2\zeta\omega_{ne}C_F \right\} \quad \text{(A-6)}$$

$$\left. K_{ie} = \omega_{ne}^2 C_F \right\} \quad \text{(A-7)}$$

In this paper, the PI controllers of both current and voltage control loops are designed by using (A-3), (A-4), (A-6), and (A-7). It can be seen that the controllers depend on the system parameters, damping ratio ζ, and the bandwidths of current loop ω_{ni} and voltage loop ne. The PI parameters in Table I of Section IV (classical method) are designed by selecting $\zeta = 0.8$, $\omega_{ni} = 2\pi \times 50$ rad/s, and $\omega_{ne} = 2\pi \times 10$ rad/s.

References

[1] D. Puangdownreong, K-N. Areerak, A. Srikaew, S. Sujijorn and P. Totarong, "System Identification via Adative Tabu Search," In *Proceedings IEEE International Conferenc on Industrial Technology (ICIT02)*, pp.915–920, 2002.

[2] S. Sujitjorn, T. Kulworawanichpong and D. Puangdownreong and K-N Areerak, "Adaptive Tabu Search and Applications in Engineering Design," *Book Chapters in Integrated Intelligent Systems for Engineering Design (ed. X. F. Zha and R..J. Howlett)*, IOS Press, The Netherlands, pp. 233–257, 2006.

[3] D. Puangdownreong, K-N. Areerak, K-L. Areerak, T. Kulworawanichpong, and S. Sujitjorn, "Application of adaptive tabu search to system identification," *IASTED International Conference on Modelling*, Identification, and Control (MIC2005), Innsbruck, Austria: February 16-18, pp.178–183, 2005.

[4] T. Kulworawanichpong, K-L. Areerak, K-N. Areerak, P. Pao-la-or, D. Puangdownreong, and S. Sujitjorn, "Dynamic parameter identification of induction motors using intelligent search techniques," *IASTED International Conference on Modelling*, Identification, and Control (MIC2005), Innsbruck, Austria: February 16-18, pp.328-332, 2005.

[5] T. Kulworawanichpong, K-L. Areerak, K-N. Areerak, and S. Sujitjorn, "Harmonic Identification for Active Power Filters Via Adaptive Tabu Search Method," *LNCS (Lecture Notes in Computer Science)* , Springer-Verlag Heidelberg, vol. 3215, pp. 687–694, 2004.

[6] K-N. Areerak, T. Kulworawanichpong and S. Sujitjorn, "Moving Towards a New Era of Intelligent Protection through Digital Relaying in Power Systems," *Lecture Notes in Computer Science*, Springer-Verlag Heidelberg, vol. 3213, , pp. 1255–1261,2004

[7] T. Narongrit, K-L. Areerak, and K-N. Areerak, "Design of an Active Power Filter using Genetic Algorithm Technique," *The 9^{th} WSEAS International Conference on Artificial Intelligent, Knowledge Engineering and Data Bases (AIKED'10)*, Cambridge, United Kingdom, pp.46–50,February 20-22, 2010.

[8] U. Leeton, D. Uthitsunthorn, U. Kwannetr, N. Sinsuphun, T. Kulworawanichpong, "Power loss minimization using optimal power flow based on particle swarm optimization," *International Conference on Electrical Engineering/Electronics Computer Telecommunications and Information Technology (ECTI-CON)*, pp. 440–444,Chaing Mai, May 19-21 2010.

[9] G. Lirui, H. Limin, Z. Liguo, L. Weina, and H. Jie, "Reactive Power Optimization for sidtribution systems based on Dual Population Ant

Colony Optimization," in *Proc. 27th Chinese Control Conference (CCC 2008).*, China, pp. 89–93, 2008.

[10] K-N. Areerak, S.V. Bozhko, G.M. Asher, and D.W.P. Thomas, . "DQ-Transformation Approach for Modelling and Stability Analysis of AC-DC Power System with Controlled PWM Rectifier and Constant Power Loads," in *Proc. 13th International Power Electronics and Motion Control Conference (EPE-PEMC 2008).*, Poznan, Poland, 2008.

[11] K-N. Areerak, S.V. Bozhko, G.M. Asher, and D.W.P. Thomas, "Stability Analysis and Modelling of AC-DC System with Mixed Load Using DQ-Transformation Method," in *Proc. IEEE International Symposium on Industrial Electronics (ISIE08).*, Cambridge, UK, pp. 19–24,2008.

[12] K-N. Areerak, S. Bozhko, G. Asher, L.de Lillo, A. Watson, T. Wu, and D.W.P. Thomas, "The Stability Analysis of AC-DC Systems including Actuator Dynamics for Aircraft Power Systems," *13th European Conference on Power Electronics and Applications (EPE 2009)*, Barcelona, Spain, 2009.

[13] K. Chaijarurnudomrung, K-N. Areerak, and K-L. Areerak, "Modeling of Three-phase Controlled Rectifier using a DQ method," *International Conference on Advances in Energy Engineering (ICAEE 2010)*, pp.56–59,2010.

Koson Chaijarurnudomrung was born in Suphaburi, Thailand, in 1986. He received the B.S. degree in electrical engineering from Suranaree University of Technology (SUT), Nakhon Ratchasima, Thailand, in 2008, where he is currently studying toward the M.S. degree in electrical engineering. His main research interests include stability analysis, modeling of power electronic system, and AI application.

Kongpan Areerak received the B.Eng. and M.Eng degrees from Suranaree University of Technology (SUT), Nakhon Ratchasima, Thailand, in 2000 and 2001, respectively and the Ph.D. degree from the University of Nottingham, Nottingham, UK., in 2009, all in electrical engineering. In 2002, he was a Lecturer in the Electrical and Electronic Department, Rangsit University, Thailand. Since 2003, he has been a Lecturer in the School of Electrical Engineering, SUT. He received the Assistant Professor in Electrical Engineering in 2010. His main research interests include system identifications, artificial intelligence application, stability analysis of power systems with constant power loads, modeling and control of power electronic based systems, and control theory.

Kongpol Areerak received the B.Eng, M.Eng, and Ph.D. degrees in electrical engineering from Suranaree University of Technology (SUT), Thailand, in 2000, 2003, and 2007, respectively. Since 2007, he has been a Lecturer and Head of Power Quality Research Unit (PQRU) in the School of Electrical Engineering, SUT. He received the Assistant Professor in Electrical Engineering in 2009. His main research interests include active power filter, harmonic elimination, AI application, motor drive, and intelligence control system.

Umaporn Kwannetr was born in Bansang, Thailand, on November 9, in 1986. She received the B.Eng. in Electrical Engineering, Suranaree University of Technology, Nakhon Ratchasima,, Thailand, in 2009. Currently she is pursuing the master degree at the University of Nakhon Ratchasima, Thailand. Her interests include the application of artificial intelligence techniques to power system optimization problems.